Firing-rate response of linear and nonlinear integrate-and-fire neurons to modulated current-based and conductance-based synaptic drive

Magnus J. E. Richardson*
Warwick Systems Biology Centre, University of Warwick, Coventry CV4 7AL, United Kingdom
(Received 11 May 2007; published 20 August 2007)

Integrate-and-fire models are mainstays of the study of single-neuron response properties and emergent states of recurrent networks of spiking neurons. They also provide an analytical base for perturbative approaches that treat important biological details, such as synaptic filtering, synaptic conductance increase, and voltage-activated currents. Steady-state firing rates of both linear and nonlinear integrate-and-fire models, receiving fluctuating synaptic drive, can be calculated from the time-independent Fokker-Planck equation. The dynamic firing-rate response is less easy to extract, even at the first-order level of a weak modulation of the model parameters, but is an important determinant of neuronal response and network stability. For the linear integrate-and-fire model the response to modulations of current-based synaptic drive can be written in terms of hypergeometric functions. For the nonlinear exponential and quadratic models no such analytical forms for the response are available. Here it is demonstrated that a rather simple numerical method can be used to obtain the steady-state and dynamic response for both linear and nonlinear models to parameter modulation in the presence of current-based or conductance-based synaptic fluctuations. To complement the full numerical solution, generalized analytical forms for the high-frequency response are provided. A special case is also identified—time-constant modulation—for which the response to an arbitrarily strong modulation can be calculated exactly.

DOI: 10.1103/PhysRevE.76.021919 PACS number(s): 87.19.La, 05.10.Gg, 05.40.−a, 87.18.Sn

I. INTRODUCTION

Integrate-and-fire models of spiking neurons, dating back to the work of Lapicque in 1907 [1], provide a tractable approximation to neuronal electrophysiology in which the cell membrane is modeled by a capacitance and a leak conductance in parallel, together with a threshold for spike generation. The coupling of a voltage dynamics to a model for fluctuating synaptic drive [2,3] has provided a versatile description of the firing-rate response during *in vivo*–like conditions; it has been extensively studied over the past half-century and continues to be a very active field of research (see [4–6] for recent reviews). The stochastic voltage dynamics induced by the fluctuating synaptic drive necessitates a probabilistic description in which distributions of voltages and firing rates are considered. One advantage of this population-density approach is that it lends itself readily to the description of ensembles of neurons [7–9] and is therefore applicable to the analysis of network states.

A standard method used for the treatment of stochastic synaptic drive is the diffusion approximation—valid in the limit of high rates of arrival of excitatory and inhibitory synaptic pulses. In this approximation, the dynamics of the voltage distribution is governed by the Fokker-Planck equation [10] from which both the voltage distributions and firing rates of neuronal ensembles can in principle be extracted [7,11,12]. The Fokker-Planck formalism provides a robust framework that has allowed the basic integrate-and-fire dynamics to be generalized to include biological details such as synaptic filtering [13–15], synaptic correlations [16], synaptic conductance [11,17–19], nonlinear response properties near the spike onset [20–24], and the dynamic effects of additional voltage-activated currents [25–27].

The full solution of the Fokker-Planck equation for arbitrary time-dependent inputs is hard to extract analytically, even for simple models with a single state variable, because it requires the solution of a two-variable partial differential equation. For this reason a common method has been to consider the effect of a weak oscillatory modulation of the synaptic input and to expand the Fokker-Planck equation order-by-order in a series in the modulated parameter (an approach taken early on for the examination of the neuronal response to noiseless current modulation [28]). The first-order solution of such expansions gives a good approximation of the dynamic response around the steady state and is a quantity that has found widespread application in the calculation of the phase diagrams of networks of neurons and the onset frequency of oscillations [7,8], the transmission of rapid signals [29–31], and spike-train power spectra [32]. However, even the first-order solution can be difficult to obtain—analytical solutions are only available for the leaky integrate-and-fire neuron under current-based synaptic modulation [7,33] in terms of hypergeometric functions. In practice, these hypergeometric functions then need to be evaluated numerically, which itself is not always trivial. Moreover, for the case of conductance-based synaptic drive, or for complex integrate-and-fire neurons such as the exponential and quadratic models, no closed analytical forms are available.

Here a simple scheme is presented that allows for the direct numerical derivation of the first-order dynamics, without requiring an intermediate analytical solution. It is as straightforward to apply to nonlinear models receiving modulated current or conductance-based synaptic drive as it is to the standard leaky model. The derivation of this method is the central result of this paper and is presented in Sec. II.

*magnus.richardson@warwick.ac.uk

In the following sections, examples are given for the application of this method to both leaky and nonlinear models. The high-frequency asymptotics are also extracted in analytic form and compared with the numerical solutions. In the next section, the general framework for the steady-state and first-order descriptions is presented. In Sec. III the case of current-based synaptic drive is treated and in Sec. IV the analysis is extended to conductance-based synaptic drive. Technical details of the numerical implementation are given in the Appendices, together with the analytical derivation of the high-frequency asymptotics. Further applications and extensions of the methodology are considered in the Discussion section.

II. GENERAL CONSIDERATIONS

Common to all probabilistic treatments of voltage trajectories in neuronal ensembles is the *continuity equation*. This relates the probability density P of finding a neuron near a voltage V to the current J of neurons whose dynamics brings them past a voltage V at a time t

$$\frac{\partial P}{\partial t} + \frac{\partial J}{\partial V} = 0. \tag{1}$$

For the models considered in this paper the synaptic drive is treated in the diffusion approximation. The dynamics of the probability density therefore obeys a Fokker-Planck equation [10] which takes the form

$$\frac{\partial P}{\partial t} = \mathcal{L}P. \tag{2}$$

The operator $\mathcal{L}$ contains derivatives up to second order in voltage. Its form depends on the underlying neuronal dynamics which are governed by some set of parameters $\{\alpha,\beta,\gamma,\ldots\}$ which, for example, could be the synaptic noise strength, rate of excitatory input, etc.

Comparison of Eqs. (1) and (2) leads to the identification of a current operator $\mathcal{J}$

$$\mathcal{J}P = J, \tag{3}$$

which is an operator comprising a first-order derivative of voltage, as can be deduced from its relation to the Fokker-Planck operator $\mathcal{L}$.

The spike and reset of the model is accounted for by boundary conditions that deal with the process of spike emission. These conditions comprise a threshold at V_{th} and a reset to V_{re}, though the exact interpretation of the threshold differs between linear and nonlinear models. The threshold and reset impose the following boundary conditions on the probability density and current

$$P(V_{\mathrm{th}-},t) = P(V_{\mathrm{re}+},t) - P(V_{\mathrm{re}-},t) = 0, \tag{4}$$

$$J(V_{\mathrm{th}-},t) = J(V_{\mathrm{re}+},t) - J(V_{\mathrm{re}-},t) = r(t), \tag{5}$$

where the $\pm$ subscripts denote the limit taken towards the value from below $(-)$ or above $(+)$ and the current just below threshold is equivalent to the firing rate $r(t)$. For future convenience, in the numerical solutions of the system a further condition, restricting the voltage to be above a lower bound V_{lb}, is also enforced

$$J(V_{\mathrm{lb}},t) = 0. \tag{6}$$

Here V_{lb} is chosen to be sufficiently negative that its precise value has a negligible impact on the evaluation of the firing rate and probability density (here $V_{\mathrm{lb}}=-100$ mV). However, certain alternatives to the classical IF model [17,34,35] include this boundary explicitly to approximate the effect of the inhibitory reversal potential; for such cases, a higher value of V_{lb} should be chosen.

A. Treatment of a weak modulation

The case of a weak perturbation is now considered in which one of the parameters, α is varied cosinusoidally at an angular frequency ω

$$\alpha(t) = \alpha_0 + \alpha_1 \cos(\omega t). \tag{7}$$

This leads to variations in all state variables that, to first order in α_1, are also cosinusoidal with a phase shift:

$$P(V,t) = P_0(V) + P_\alpha(V)\cos[\omega t + \psi_\alpha(V)], \tag{8}$$

$$J(V,t) = J_0(V) + J_\alpha(V)\cos[\omega t + \gamma_\alpha(V)], \tag{9}$$

$$r(t) = r_0 + r_\alpha \cos(\omega t + \rho_\alpha). \tag{10}$$

It proves convenient to consider an allied system which is driven by a sinusoidal drive so that the effect of the modulation can be written in complex form, greatly simplifying the treatment. For example,

$$r_\alpha \cos(\omega t + \rho_\alpha) + i r_\alpha \sin(\omega t + \rho_\alpha) = \hat{r}_\alpha e^{i\omega t}. \tag{11}$$

The amplitude r_α and phase ρ_α of the complex $\hat{r}_\alpha$, as well as those for $\hat{P}_\alpha$ and $\hat{J}_\alpha$, together characterize the response properties to a modulation of the parameter α.

The Fokker-Planck equations for the steady-state and dynamic perturbations may be written in the form

$$0 = \mathcal{L}_0 P_0 \quad \text{and} \quad i\omega\hat{P}_\alpha = \mathcal{L}_0\hat{P}_\alpha + \frac{\partial F_\alpha}{\partial V}, \tag{12}$$

where $\mathcal{L}_0$ is the Fokker-Planck operator with all its parameters $\{\alpha_0,\beta_0,\gamma_0,\ldots\}$ set at their steady-state values. The inhomogeneous term F_α is defined by

$$F_\alpha = -\mathcal{J}_\alpha P_0 \quad \text{where } \mathcal{J}_\alpha = \alpha_1 \left.\frac{\partial \mathcal{J}}{\partial \alpha}\right|_{\alpha=\alpha_0}. \tag{13}$$

The notation is a little heavy at this stage due to the requirement of treating the problem generally. It simplifies considerably as soon as a specific case is considered.

B. Method for the numerical solution

The strategy essentially involves breaking the Fokker-Planck equation into two simultaneous first-order equations for the current J and probability density P. These equations

can then be solved by appropriately separating out subsolutions and starting the integration from a convenient point.

The steady-state solution is first constructed by resolving the Fokker-Planck equation into the form

$$-\frac{\partial J_0}{\partial V} = r_0[\delta(V - V_{\text{th}}) - \delta(V - V_{\text{re}})], \tag{14}$$

$$\mathcal{J}_0 P_0 = J_0, \tag{15}$$

with the boundary conditions (5) included explicitly in the first equation. Both the current and probability density are proportional to the unknown firing rate r_0, so the substitutions

$$J_0 = r_0 j_0 \quad \text{and } P_0 = r_0 p_0 \tag{16}$$

allow for the firing rate to be canceled from the pair of equations (14) and (15). The resulting equations for j_0 and p_0 can then be integrated numerically backwards, from the threshold V_{th} to the lower bound V_{lb}, with initial conditions $j_0(V_{\text{th}})=1$ and $p_0(V_{\text{th}})=0$. The firing rate r_0 is found by noting that the total probability density integrates to one; hence r_0 is equal to the reciprocal of the integral of p_0 over the voltage range. The correctly scaled current J_0 and probability density P_0 are then obtained from Eq. (16). An example of this method is given in Appendix A in a form suitable for numerical integration.

The dynamic response can be found similarly. In this case, the pair of first-order equations to be solved are

$$-\frac{\partial \hat{J}_\alpha}{\partial V} = i\omega \hat{P}_\alpha + \hat{r}_\alpha[\delta(V - V_{\text{th}}) - \delta(V - V_{\text{re}})], \tag{17}$$

$$\mathcal{J}_0 \hat{P}_\alpha = \hat{J}_\alpha + F_\alpha. \tag{18}$$

The firing-rate modulation $\hat{r}_\alpha$ is again unknown and the second equation now contains the inhomogeneous term F_α. The method is to separate the solution into two components by making the substitutions

$$\hat{J}_\alpha = \hat{r}_\alpha \hat{\mathrm{J}}_r + \alpha_1 \hat{\mathrm{J}}_\alpha \quad \text{and } \hat{P}_\alpha = r_\alpha \hat{p}_r + \alpha_1 \hat{p}_\alpha. \tag{19}$$

The pair of functions $\hat{\mathrm{J}}_r$ and $\hat{p}_r$ satisfy equations (17) and (18) with $\alpha_1=0$ (i.e., $F_\alpha=0$),

$$-\frac{\partial \hat{\mathrm{J}}_r}{\partial V} = i\omega \hat{p}_r + \delta(V - V_{\text{th}}) - \delta(V - V_{\text{re}}), \tag{20}$$

$$\mathcal{J}_0 \hat{p}_r = \hat{\mathrm{J}}_r, \tag{21}$$

with boundary conditions $\hat{\mathrm{J}}_r(V_{\text{th}})=1$, $\hat{p}_r(V_{\text{th}})=0$. It can be noted that these solutions are not specific to the parameter being modulated. The second pair of functions $\hat{\mathrm{J}}_\alpha$ and $\hat{p}_\alpha$ account for the inhomogeneous driving term $F_\alpha=\alpha_1 f_\alpha$ and satisfy equations (17) and (18) with $\hat{r}_\alpha=0$,

$$-\frac{\partial \hat{\mathrm{J}}_\alpha}{\partial V} = i\omega \hat{p}_\alpha, \tag{22}$$

$$\mathcal{J}_0 \hat{p}_\alpha = \hat{\mathrm{J}}_\alpha + f_\alpha, \tag{23}$$

with boundary conditions $\hat{\mathrm{J}}_\alpha(V_{\text{th}})=0$, $\hat{p}_\alpha(V_{\text{th}})=0$.

Both these pairs of equations are coupled first-order differential equations and can be integrated numerically from the threshold V_{th} to V_{lb}. The final trick is to extract the firing-rate modulation $\hat{r}_\alpha$ using the condition (6) together with the definition for the current (19) to yield

$$\hat{r}_\alpha = -\alpha_1 \frac{\hat{\mathrm{J}}_\alpha(V_{\text{lb}})}{\hat{\mathrm{J}}_r(V_{\text{lb}})}. \tag{24}$$

This can then be used with the definitions given in equation set (19) to yield the modulated probability density and current, if required.

This is the central result of the paper. The method just described works equally well for linear or nonlinear IF models and current or conductance-based noise; the only difference being the form of the current operator $\mathcal{J}$ and the interpretation of the voltage threshold. In the remainder of the paper these cases are considered in turn and analytical formulae for the high-frequency asymptotics also derived.

III. CURRENT-DRIVEN MODELS

In this section, the response properties of neurons receiving additive noise—a fluctuating current—are examined. It should be noted that this covers both current-based synaptic drive and conductance-based synaptic drive treated in the Gaussian approximation [36,37]—the key point being that the noise is additive. In the Gaussian approximation the tonic conductance is absorbed into an increased membrane conductance, but the higher-order multiplicative noise is neglected. The classical leaky integrate-and-fire model, for which many properties of the response to weak stimuli are known analytically, is first presented. A special case is also identified for which an exact solution to an arbitrarily strong modulation can be found. The more general case of nonlinear integrate-and-fire models, such as the exponential or algebraic IF models (like the quadratic IF model) are then considered. For the LIF and EIF the results of the numerical solutions are given in Figs. 1 and 2. For all cases a general formula for the high-frequency response is given and the specific cases of current, noise and conductance modulation given explicitly. For the EIF the effect of modulating the spike-generating parameters is also considered.

A. Leaky IF model

The Langevin equation for the linear IF model of a neuron with capacitance C and total conductance g can be written in the form

$$\tau \frac{dV}{dt} = E - V + \sigma\sqrt{2\tau}\xi(t), \tag{25}$$

where $\tau=C/g$ is the membrane time constant and $\xi(t)$ is zero-mean, delta-correlated Gaussian white noise $\langle \xi(t)\xi(t')\rangle = \delta(t-t')$. For convenience, the noise strength has been pa-

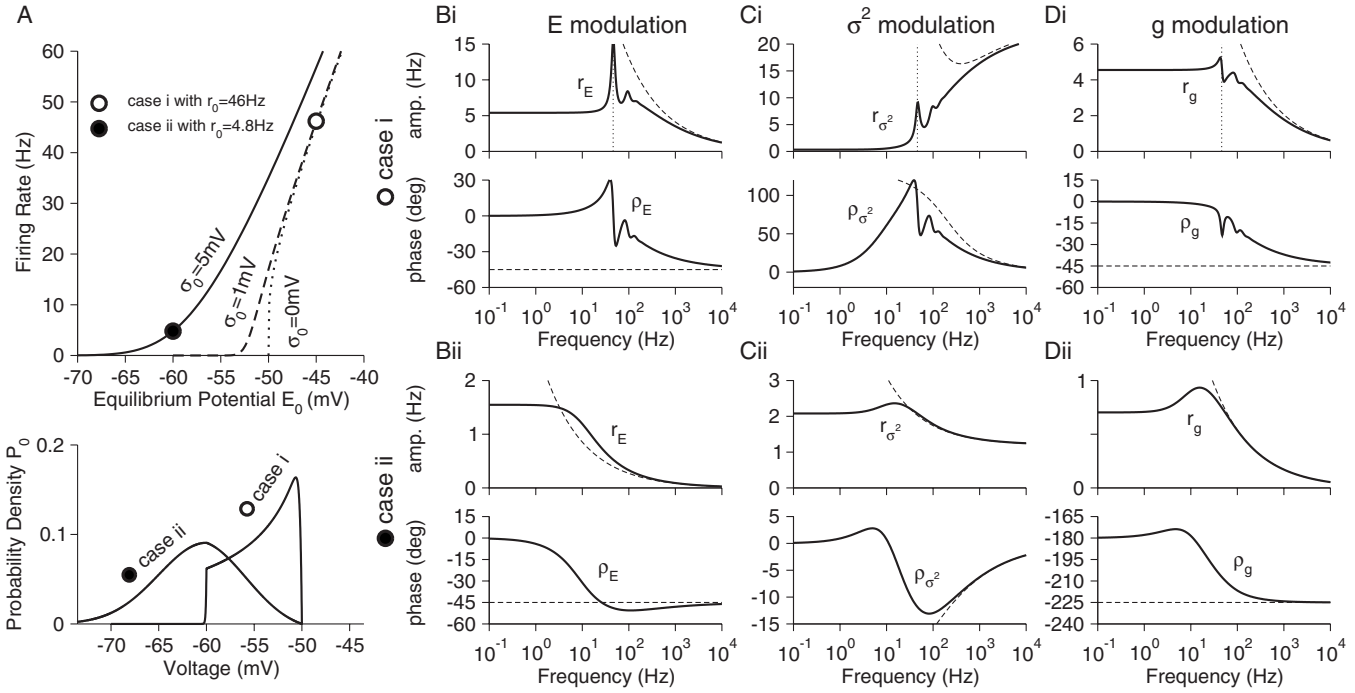

FIG. 1. Firing-rate response of the leaky IF model. (A) Top panel: Steady-state firing rate r_0 as a function of the resting potential E_0 for three different strengths of the noise σ_0. Two cases are used to examine the modulation: (i) Suprathreshold excitation with near-deterministic firing ($E_0=-45$ mV; $\sigma_0=1$ mV; $r_0=46$ Hz) and (ii) subthreshold excitation with noise-driven firing ($E_0=-60$ mV; $\sigma_0=5$ mV; $r_0=4.8$ Hz). (A) Lower panel: Steady-state probability densities P_0. In panels (B)–(D) the bold lines are numerical solutions and the dashed lines high-frequency asymptotics. (B) Current E modulation. (Bi) Case i with $E_1=1$ mV: Resonances are seen at the firing rate (dotted line) and its harmonics, characteristic of low background noise. (Bii) Case ii with $E_1=1$ mV. In both cases i and ii the phase asymptote is $-45°$ (dashed lines). (C) Variance σ^2 modulation. (Ci) Case i with $\sigma_1^2=0.5$ mV^2: Again there are resonances at a modulation frequency equal to the firing rate and its harmonic. (Cii) Case ii with $\sigma_1^2=6.25$ mV^2: A resonance and phase zero are seen near 10 Hz. In both cases i and ii the amplitude r_{σ^2} is nonzero and the phase shift ρ_{σ^2} vanishes for high frequency. (D) Conductance g modulation. (Di) Case i with $g_1/g_0=0.1$. The phase asymptote [Eq. (36)] is $-45°$ because $E_0>V_{\mathrm{th}}$. (Dii) Case ii with $g_1/g_0=0.2$ which also shows a broad resonance near 10 Hz. Here the asymptote is $-225°\equiv 135°$ because $E_0<V_{\mathrm{th}}$. Parameters used were $V_{\mathrm{th}}=-50$ mV, $V_{\mathrm{re}}=-60$ mV, $V_{\mathrm{lb}}=-100$ mV, and $\tau_0=20$ ms. The integration step was 10 μV.

rametrized in terms of the induced voltage variance σ^2 (in absence of threshold). This necessitates the τ factor appearing in the noise term, but does not imply that the strength of the synaptic noise is itself a function of τ or the conductance g.

For an ensemble of identical neurons with different realizations of the noise $\xi(t)$, Eq. (25) leads to the Fokker-Planck equation [10]

$$\frac{\partial P}{\partial t}=\frac{\sigma^2}{\tau}\frac{\partial^2 P}{\partial V^2}+\frac{\partial}{\partial V}\left(\frac{(V-E)}{\tau}P\right) \tag{26}$$

with an associated current operator $\mathcal{J}$ of the form

$$\mathcal{J}=\frac{E-V}{\tau}-\frac{\sigma^2}{\tau}\frac{\partial}{\partial V}. \tag{27}$$

For the case of the LIF the steady-state equations (14) and (15) can therefore be written as

$$-\frac{\partial J_0}{\partial V}=r_0[\delta(V-V_{\mathrm{th}})-\delta(V-V_{\mathrm{re}})], \tag{28}$$

$$-\frac{\partial P_0}{\partial V}=\frac{\tau_0}{\sigma_0^2}\left(\frac{(V-E_0)}{\tau_0}P_0+J_0\right). \tag{29}$$

The numerical method required for the solution of equations (28) and (29) is straightforward (a convenient scheme is given in Appendix A). In Fig. 1(a) the firing rate as a function of E_0 and two examples of the probability densities are given for the steady-state of the leaky IF model.

The response to modulations of some parameter α can now be considered: The modulation equations (17) and (18) are

$$-\frac{\partial \hat{J}_\alpha}{\partial V}=i\omega\hat{P}_\alpha+\hat{r}_\alpha[\delta(V-V_{\mathrm{th}})-\delta(V-V_{\mathrm{re}})], \tag{30}$$

$$-\frac{\partial \hat{P}_\alpha}{\partial V}=\frac{\tau_0}{\sigma_0^2}\left(\frac{(V-E_0)}{\tau_0}\hat{P}_\alpha+\hat{J}_\alpha+F_\alpha\right) \tag{31}$$

for the LIF model. The general formula for the high-frequency asymptotics of the LIF can also be calculated as a function of the driving term F_α (see Appendix B 1) and shown to be

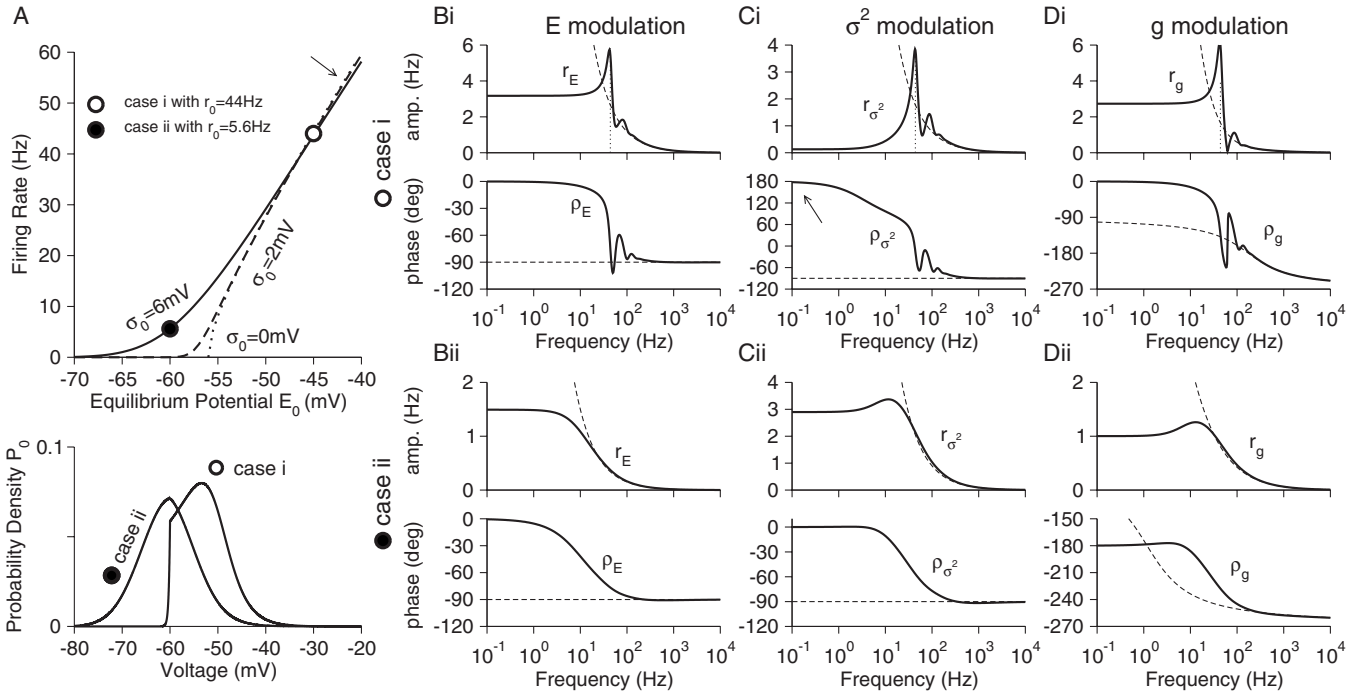

FIG. 2. Firing-rate response of the exponential IF model. (A) Top panel: Steady-state firing rate r_0 as a function of the resting potential E_0 for three different strengths of noise σ_0. Note that for E_0 greater than about −47 mV increasing noise decreases the firing rate. Two cases are used to examine the modulation: (i) Near-deterministic firing (E_0=−45 mV; σ_0=2 mV; r_0=44 Hz) and (ii) noise-driven firing (E_0=−60 mV; σ_0=6 mV; r_0=5.6 Hz). (A) Lower panel: Steady-state probability densities P_0. In panels (B)–(D) bold lines are numerical solutions and dashed lines the high-frequency asymptotics. (B) Current E modulation. (Bi) Case i with E_1=1 mV: Resonances can be seen at the firing rate (dotted line) and its harmonics. (Bii) Case ii with E_1=1 mV. In both cases i and ii the phase asymptotes (dashed lines) are at −90°. (C) Variance σ^2 modulation. (Ci) Case i with σ_1^2=2 mV^2: Again there are resonances at a modulation frequency equal to the firing rate and its harmonic. Here the modulation at low frequency is 180° (see arrow) due to the negative impact of noise on higher firing rates [panel (A), arrow]. (Cii) Case ii σ_1^2=18 mV^2: A resonance and phase zero are seen at ~10 Hz. In all cases of current and variance modulation the asymptotes [dashed lines, equation set (51)] decay with the reciprocal of frequency. (D) Conductance g modulation. (Di) Case i with g_1/g_0=0.1. The phase asymptote [Eq. (52)] is −270° equivalent to a 90° phase advance. (Dii) Case ii with g_1/g_0=0.2 shows a broad resonance at 10 Hz. A slow, logarithmic relaxation to the high-frequency limit can be seen in all (D) panels. Parameters were V_T=−53 mV, Δ_T=3 mV, $V_{\rm th}$=0 mV, $V_{\rm re}$=−60 mV, $V_{\rm lb}$=−100 mV, and τ_0=20 ms with integration step 10 μV.

$$\hat{r}_\alpha = e^{-i\pi/4}\sqrt{\frac{\sigma_0^2}{\omega\tau_0}}\left.\frac{\partial F_\alpha}{\partial V}\right|_{\rm th} - F_\alpha(V_{\rm th}). \tag{32}$$

Three forms of modulation will now be considered: modulation of the resting potential E, which is equivalent to a modulated input current, modulation of the noise variance σ^2, and modulation of the leak conductance g. From the definition of F_α given in Eq. (13) and the form of the current operator $\mathcal{J}$ for the LIF (27), the corresponding driving terms are

$$F_E = -\frac{E_1}{\tau_0}P_0, \quad F_{\sigma^2} = \frac{\sigma_1^2}{\tau_0}\frac{\partial P_0}{\partial V},$$

and

$$F_g = \frac{1}{\tau_0}\frac{g_1}{g_0}(V - E_0)P_0. \tag{33}$$

Full analytical solutions have been given for cases of current [7] and variance [7,29] modulation for the LIF and the high-frequency asymptotics have been extracted from these solutions. The general formula (32) agrees with these derivations for $\hat{r}_E$ and $\hat{r}_{\sigma^2}$

$$\hat{r}_E \simeq r_0\frac{E_1}{\sigma_0}\frac{1}{\sqrt{\omega\tau_0}}e^{-i\pi/4}, \tag{34}$$

$$\hat{r}_{\sigma^2} \simeq r_0\frac{\sigma_1^2}{\sigma_0^2}\left(1 + \frac{(V_{\rm th} - E_0)}{\sigma_0\sqrt{\omega\tau_0}}e^{-i\pi/4}\right), \tag{35}$$

and also gives a new result for conductance modulation

$$\hat{r}_g \simeq r_0\frac{g_1}{g_0}\frac{(E_0 - V_{\rm th})}{\sigma_0\sqrt{\omega\tau_0}}e^{-i\pi/4}. \tag{36}$$

These asymptotic results are compared to the full numerical solutions of equations (30) and (31) in Fig. 1. It is interesting to note that, for the case of conductance modulation, the value of the high-frequency phase asymptote depends on whether the neuron is in a suprathreshold $E_0 > V_{\rm th}$ tonic-current driven firing regime or in a subthreshold $V_{\rm th} > E_0$ fluctuating-current driven firing regime.

Leaky IF response to time-constant modulation

The high-frequency limit of the conductance modulation (36) is proportional to the decaying component of the noise

modulation (35). Hence, if simultaneous conductance and noise modulations occurred with amplitudes satisfying $g_1/g_0=\sigma_1^2/\sigma_0^2$ the decaying terms would cancel to leave a constant contribution proportional to r_0. In fact this combination corresponds to a particular balanced case in which conductance and synaptic noise are both varied in such a way that the voltage variance (in absence of threshold) remains constant. This balance is equivalent to varying the time constant τ as it appears in the Fokker-Planck equation (26).

Surprisingly, the cancellation of the decaying terms continues to all orders for this form of balanced drive: The firing-rate response to an arbitrarily strong τ modulation, after initial transients have died away, can be derived exactly. The proof is as follows: By introducing the variable $s=t/\tau(t)$ the LIF Fokker-Planck equation becomes

$$\frac{\partial P}{\partial s}=\sigma_0^2\frac{\partial^2 P}{\partial V^2}+\frac{\partial}{\partial V}[(V-E_0)P]. \tag{37}$$

In this form, there is no explicit time dependence; the system equilibrates to yield a steady-state distribution P_0 and firing rate r_0 (in units of s) parametrized by the constant quantities E_0 and σ_0. On transforming back to the standard time variable t the true firing rate is found to be

$$r(t)=\frac{1}{\tau(t)}r_0(\sigma_0,E_0,\tau_0=1), \tag{38}$$

which is exact for arbitrary modulations of $\tau(t)$. In other words, because $\tau(t)$ is the only quantity carrying units of time, varying it is equivalent to compressing and stretching time.

B. Nonlinear IF models

The method outlined in the previous section can be directly applied to nonlinear integrate-and-fire models such as the exponential (EIF), quadratic (QIF), or more general algebraic (AIF) integrate-and-fire models. For this class of models the Langevin equation takes the form

$$\tau\frac{dV}{dt}=E-V+\psi+\sigma\sqrt{2\tau}\xi(t), \tag{39}$$

where ψ is the spike-generating current that dominates the dynamics for large voltages. The corresponding Fokker-Planck equation takes the form

$$\frac{\partial P}{\partial t}=\frac{\sigma^2}{\tau}\frac{\partial^2 P}{\partial V^2}+\frac{\partial}{\partial V}\left(\frac{(V-E-\psi)}{\tau}P\right), \tag{40}$$

with the current operator

$$\mathcal{J}=\frac{E-V+\psi}{\tau}-\frac{\sigma^2}{\tau}\frac{\partial}{\partial V}. \tag{41}$$

Hence, for the steady state of nonlinear models, the pair of equations is

$$-\frac{\partial J_0}{\partial V}=r_0[\delta(V-V_{\rm th})-\delta(V-V_{\rm re})], \tag{42}$$

$$-\frac{\partial P_0}{\partial V}=\frac{\tau_0}{\sigma_0^2}\left(\frac{(V-E_0-\psi)}{\tau_0}P_0+J_0\right), \tag{43}$$

where the threshold $V_{\rm th}$ is chosen to be sufficiently large that its exact value does not alter the dynamics (here 0 mV). The corresponding equations for the modulated response are

$$-\frac{\partial \hat{J}_\alpha}{\partial V}=i\omega\hat{P}_\alpha+\hat{r}_\alpha[\delta(V-V_{\rm th})-\delta(V-V_{\rm re})], \tag{44}$$

$$-\frac{\partial \hat{P}_\alpha}{\partial V}=\frac{\tau_0}{\sigma_0^2}\left(\frac{(V-E_0-\psi)}{\tau_0}\hat{P}_\alpha+\hat{J}_\alpha+F_\alpha\right). \tag{45}$$

For both the steady state and modulations the method of solution is the same as that described for the LIF, using the substitutions given in Eqs. (16) and (19), respectively.

A general solution for the high-frequency asymptotics for an arbitrary F_α can also be derived (see Appendix B 2) for the nonlinear case

$$\hat{r}_\alpha=\frac{1}{i}\lim_{s\to 0}\int_0^\infty dm\, e^{-(i+s)m}F_\alpha(m), \tag{46}$$

where $F_\alpha(m)$ is expressed in terms of a variable m which satisfies

$$\frac{dm}{dV}=-\frac{\omega\tau_0}{\psi} \tag{47}$$

so that the form of m depends on which nonlinear IF model is being considered. These forms will be given below for the cases of exponential and algebraic spike currents and used to determine analytical solutions for the high-frequency response.

C. Exponential IF response to modulation

The exponential IF model [23,31] captures the initial dynamics of the opening of the spike-generating sodium channels. In this approximation the spike-generating current takes the form

$$\psi=\Delta_T e^{(V-V_T)/\Delta_T}, \tag{48}$$

where V_T sets the voltage scale at which the exponential term becomes significant and Δ_T is a measure of the sharpness of the spike. Some examples of the steady-state firing rate and distributions are given in Fig. 2.

To calculate the high-frequency asymptotics the quantity m given in Eq. (47) must be derived. For the EIF it takes the form

$$m=\omega\tau_0\Delta_T/\psi. \tag{49}$$

From Eq. (43) it is seen that $P_0\simeq r_0\tau_0/\psi$ in the large V, large ψ limit. Using this result in combination with Eq. (49) the quantities F_α given in equation set (33) can be rewritten as functions of m to give

$$F_E=-m\frac{E_1 r_0}{\Delta_T\omega\tau_0},\quad F_{\sigma^2}=-m\frac{\sigma_1^2 r_0}{\Delta_T^2\omega\tau_0},$$

and

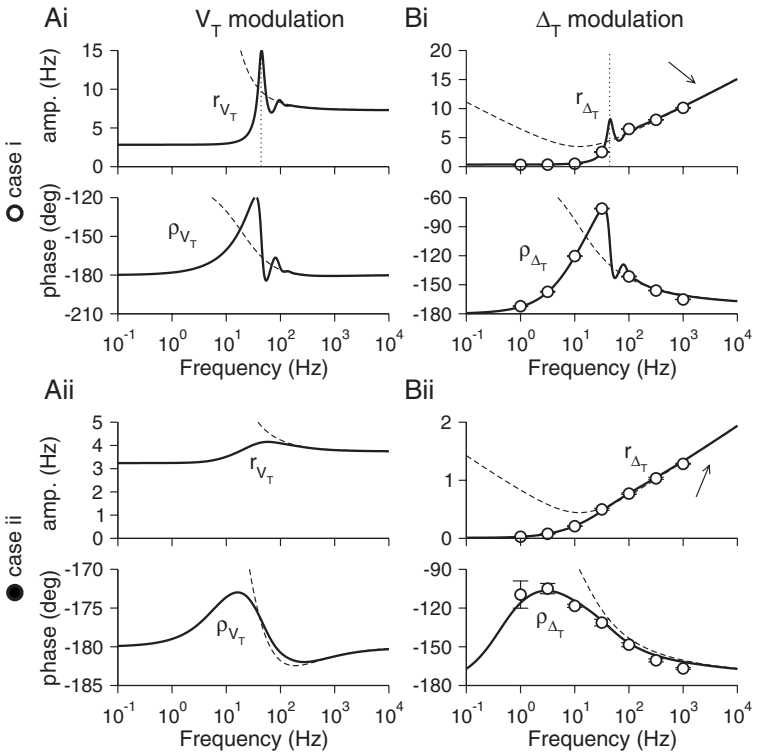

FIG. 3. Firing-rate response of the exponential IF model to modulations of spike-generating parameters. Cases i and ii defined in Fig. 2 are used with the same EIF parameters. Bold lines are numerical solutions and dashed lines high-frequency asymptotics. (A) Modulation of the spike threshold V_T. (Ai) For near-deterministic firing, with $V_{T1}=0.5$ mV, a resonance in the response is seen at the firing rate $r_0 \simeq 44$ Hz. The asymptote is a constant with a 180° phase. (Aii) The noise-driven case with $V_{T1}=2$ mV. A broad resonance is seen near 100 Hz with the asymptote again becoming constant with a 180° phase lag. (B) Modulation of the spike width Δ_T. Symbols show results from Monte Carlo simulations (see main text). (Bi) For the near-deterministic case with $\Delta_{T1}=0.15$ mV there is again a resonance equal to the firing rate r_0. It should be noted that the response amplitude *increases* with increasing frequency (see arrows). (Bii) The noise-driven case with $\Delta_{T1}=0.15$ mV; increasing response to high-frequency modulation can again be seen.

$$F_g = m\frac{g_1 r_0}{g_0 \omega}\left(\log(\omega\tau_0) + \frac{V_T - E_0}{\Delta_T} - \log(m)\right). \quad (50)$$

These can be integrated in Eq. (46) to yield the firing-rate modulations. For the mean and variance the modulations were previously derived [31] using a method that is a special case of Eq. (46) and take the form

$$\hat{r}_E \simeq \frac{r_0}{i\omega\tau_0}\frac{E_1}{\Delta_T} \text{ and } \hat{r}_{\sigma^2} \simeq \frac{r_0}{i\omega\tau_0}\frac{\sigma_1^2}{\Delta_T^2}. \quad (51)$$

For both cases the amplitudes decay as $1/\omega$ with a phase difference of −90°. These asymptotes are included in Fig. 2 together with the numerical solutions. For the case of conductance-based modulation the decay is marginally weaker, the $1/\omega$ being moderated by a logarithmic factor

$$\hat{r}_g \simeq \frac{g_1}{g_0}\frac{ir_0}{\omega\tau_0}\left(\log(\omega\tau_0) + \frac{V_T - E_0}{\Delta_T} + \frac{i\pi}{2} + \gamma - 1\right), \quad (52)$$

where $\gamma=0.57722\ldots$ is Euler's constant. The phase asymptote here is reversed to give a lead of 90°. Two examples of this response are also given in Fig. 2.

For the EIF model there are two further quantities that might be varied: The spike-generating parameters V_T and Δ_T. Though it is not clear what biological mechanisms might lead to direct modulations of these quantities, it should be remembered that in practice the parameters V_T, Δ_T represent averages over the combined dynamics of the m, h, and n voltage-activated variables of the underlying Hodgkin-Huxley currents [38]. Any of the modulations previously considered, that affect the average voltage, might be expected to induce secondary modulations in the spike-generating parameters (if some model for the effect of the voltage modulations on V_T and Δ_T were included). For this reason, an examination of the effect of a modulation of these effective parameters is worthwhile. The corresponding driving terms are

$$F_{V_T} = \frac{V_{T1}}{\Delta_T} r_0 \tau_0, \quad F_{\Delta_T} = \frac{\Delta_{T1}}{\Delta_T}(\log \omega\tau_0 - \log m - 1), \quad (53)$$

leading to the response modulations

$$\hat{r}_{V_T} \simeq -r_0\frac{V_{T1}}{\Delta_T}, \quad \hat{r}_{\Delta_T} \simeq -r_0\frac{\Delta_{T1}}{\Delta_T}\log(\omega\tau_0), \quad (54)$$

which are given here to leading order. It is notable that neither response decays with frequency. The case of V_T modulation is similar to noise modulation in the LIF and, if correctly combined with modulation of the conductance and noise, an exact solution equivalent to the τ modulation in Eq. (38) is found for the EIF. The response to Δ_T modulation actually *grows* with frequency and, though for very high frequencies this unbounded behavior would presumably be curtailed by higher-order terms, the asymptotic limit and numerically-generated response plotted in Fig. 3, panels (Bi) and (Bii), agree well with Monte Carlo simulations up to frequencies of 1000 Hz. Only at the highest frequencies are weak nonlinear effects, due to the strong amplification, seen in the phase. (Simulations were made with a forward Euler scheme, time step in the range 5–100 μs, with error bars showing standard error on the mean over 10 repeated trials, each of duration in the range 20–100 s, depending on the frequency.)

Above it was stated that though it was not obvious how V_T or Δ_T might be modulated directly, they could be modulated as a side effect of the more direct modulation of an-

other parameter (given some model linking these features). Because the modulations of V_T or Δ_T do not decay with frequency, their induced modulations would be as important as the primary modulation, and hence these effects would need to be accounted for if the overall response were to be correctly calculated.

D. Asymptotic response of algebraic IF models

To complete this section the high-frequency asymptotics of models with *algebraic* spikes will also be considered. By this it is meant models that have spike generating currents that vary with some power of voltage, when the voltage is large and positive, where an important model from this class is the quadratic integrate-and-fire model [20–24]. For algebraic IF models the spike-generating current scales as

$$\psi \simeq \Delta_T \left(\frac{V - V_T}{\Delta_T} \right)^k \tag{55}$$

for large voltages, and where in all of the following only cases where $k > 1$ are considered. It should be noted that for the following derivation of the high-frequency asymptotics it is not necessary to specify the exact form of the subthreshold dynamics.

For algebraic models the quantity m defined through Eq. (47) takes the form

$$m = \frac{\omega \tau_0}{(k-1)} \left(\frac{V - V_T}{\Delta_T} \right)^{1-k} \tag{56}$$

and from Eq. (43) for large voltage $P_0 \simeq r_0 \tau_0 / \psi$. The driving terms (33) for the AIF can therefore be written in terms of m as

$$F_E = -r_0 \frac{E_1}{\Delta_T} \left(\frac{(k-1)m}{\omega \tau_0} \right)^{k/(k-1)},$$

$$F_{\sigma^2} = -r_0 k \frac{\sigma_1^2}{\Delta_T^2} \left(\frac{(k-1)m}{\omega \tau_0} \right)^{(k+1)/(k-1)},$$

and for the case of conductance modulation, to leading order,

$$F_g = r_0 \frac{g_1}{g_0} \frac{(k-1)m}{\omega \tau_0} + r_0 \frac{g_1}{g_0} \frac{V_T - E_0}{\Delta_T} \left(\frac{(k-1)m}{\omega \tau_0} \right)^{k/(k-1)}. \tag{57}$$

These can be inserted into the integral (46) to yield the firing rate modulations. For E modulation the result is

$$\hat{r}_E \simeq r_0 \frac{E_1}{\Delta_T} \Gamma \left(\frac{2k-1}{k-1} \right) \left(\frac{k-1}{i \omega \tau_0} \right)^{k/(k-1)}, \tag{58}$$

which agrees with the $k=2$ case previously treated [31]. For σ^2 modulation the result is

$$\hat{r}_{\sigma^2} \simeq r_0 k \frac{\sigma_1^2}{\Delta_T^2} \Gamma \left(\frac{2k}{k-1} \right) \left(\frac{k-1}{i \omega \tau_0} \right)^{(k+1)/(k-1)}, \tag{59}$$

which also agrees with the case of $k=2$ previously treated [31]. Finally, the result for conductance modulation takes the form

$$\hat{r}_g \simeq -r_0 \frac{g_1}{g_0} \frac{(k-1)}{i \omega \tau_0} \tag{60}$$

to leading order. In all cases algebraic models are seen to be less responsive than the EIF, in the sense that the high-frequency asymptotes decay with a more negative power of frequency.

IV. CONDUCTANCE-DRIVEN MODELS

A full conductance-based model of synaptic drive comprises a tonic conductance change and, in contrast to the current-based noise considered in the previous section, an additional *multiplicative* noise source that depends on voltage [3]. However, a notation will be adopted that brings the analysis required into a rather similar form to the current-noise case. As will be seen, there is little qualitative difference between the response properties of neurons to parameter modulation in the presence of multiplicative conductance-based noise or additive current-based noise. The numerical method is similar and the general formulas for the high-frequency response are identical, save for the voltage dependence of the variance σ^2.

A. Leaky IF with conductance noise

A scenario is considered in which a neuron with leak conductance g_L and capacitance C receives an excitatory and inhibitory drive of amplitude a_e, a_i respectively. Using the case of purely excitatory drive as an illustration, the voltage dynamics follow

$$C \frac{dV}{dt} = g_L (E_L - V) + a_e (E_e - V) \sum_{\{t_e\}} \delta(t - t_e), \tag{61}$$

where $\{t_e\}$ is the set of pulse arrival times at rate R_e. Some care needs to be taken in defining the effect of the synaptic pulses on the voltage, because the $\delta(t)V(t)$ terms on the right-hand side are open to interpretation. Here it is considered that the δ functions represent the limit of short synaptic pulses and so it is the Stratonovich definition [10] of stochastic calculus that is chosen. For the case of excitatory drive, this implies that on the arrival of a pulse the voltage jumps from its initial value V to $V + \Delta_V$ where $\Delta_V = b_e (E_e - V)$ and $b_e = 1 - e^{-a_e}$. In any case, the diffusion approximation requires that b_e is small so that, practically speaking, the difference between a_e and b_e is also small.

The corresponding Fokker-Planck equation can now be derived [11,18,39] and written in a form similar to the current-based case, but with a voltage-dependent variance $\sigma^2(V)$, a synaptic-drive-dependent time constant τ and a drive-dependent-resting potential E. On including both excitation and inhibition, the equation reads

$$\frac{\partial P}{\partial t} = \frac{\partial^2}{\partial V^2} \left(\frac{\sigma^2}{\tau} P(V) \right) + \frac{\partial}{\partial V} \left(\frac{(V - E)}{\tau} P(V) \right), \tag{62}$$

with an associated current operator

$$\mathcal{J} = \frac{E - V}{\tau} - \frac{\partial}{\partial V}\frac{\sigma^2}{\tau}. \tag{63}$$

The terms appearing in the Fokker-Planck and current operators may be expressed in terms of the synaptic drive as follows:

$$\frac{\sigma^2}{\tau} = \frac{1}{2}[R_e b_e^2 (V - E_e)^2 + R_i b_i^2 (V - E_i)^2] \tag{64}$$

and

$$\frac{V - E}{\tau} = \frac{V - E_L}{\tau_L} + R_e b_e (V - E_e) + R_i b_i (V - E_i), \tag{65}$$

from which τ and E may be extracted

$$E = \frac{E_L + \tau_L R_e b_e E_e + \tau_L R_i b_i E_i}{1 + \tau_L R_e b_e + \tau_L R_i b_i}, \tag{66}$$

$$\tau = \frac{\tau_L}{1 + \tau_L R_e b_e + \tau_L R_i b_i}, \tag{67}$$

by collecting the prefactor of the voltage and constant terms on the right-hand side of Eq. (65).

The scheme for the numerical derivation of the steady state properties is not significantly different to the current-based case. It remains only to arrange Eq. (15) with the current operator (63) into a form convenient for integration. It is first noted that

$$\frac{\partial}{\partial V}\left(\frac{\sigma_0^2}{\tau_0}\right) + \frac{(V - E_0)}{\tau_0} = \frac{(V - E_0')}{\tau_0'}, \tag{68}$$

where the dashed quantities on the right-hand side just require the changes $b_e \to b_e + b_e^2$ in Eq. (65) and similarly for inhibition. Hence the equations required for the numerical solution are

$$-\frac{\partial J_0}{\partial V} = r_0[\delta(V - V_{\text{th}}) - \delta(V - V_{\text{re}})], \tag{69}$$

$$-\frac{\partial P_0}{\partial V} = \frac{\tau_0}{\sigma_0^2}\left(\frac{(V - E_0')}{\tau_0'} P_0 + J_0\right). \tag{70}$$

These are of the same form as the current-noise case given in Eqs. (28) and (29) except that the variance σ_0^2 is now voltage dependent. This method of calculating the firing rate and probability density is more convenient than using the analytical solutions [11,18] which themselves involve numerical integration.

The numerical derivation of the response to modulation follows similarly with the pair of equations taking the form

$$-\frac{\partial \hat{J}_\alpha}{\partial V} = i\omega \hat{P}_\alpha + \hat{r}_\alpha[\delta(V - V_{\text{th}}) - \delta(V - V_{\text{re}})], \tag{71}$$

$$-\frac{\partial \hat{P}_\alpha}{\partial V} = \frac{\tau_0}{\sigma_0^2}\left(\frac{(V - E_0')}{\tau_0'} \hat{P}_\alpha + \hat{J}_\alpha + F_\alpha\right). \tag{72}$$

For conductance-based drive the biophysical parameters that might be varied are R_e, b_e, or E_e and similarly for inhibition. Modulation of R_e has a simple interpretation in terms of modulating the presynaptic rates

$$F_{R_e} = \mathcal{R}_{e1} b_e \left(\frac{b_e}{2}\frac{\partial}{\partial V}[(V - E_e)^2 P_0] + (V - E_e) P_0\right). \tag{73}$$

Modulation of b_e can be interpreted as a simple model for the effects of synchrony in the presynaptic population

$$F_{b_e} = b_{e1} R_e \left(b_e \frac{\partial}{\partial V}[(V - E_e)^2 P_0] + (V - E_e) P_0\right) \tag{74}$$

and the modulation of E_e might arise from changes in local ionic concentrations, for example in spines upon which synapses are formed

$$F_{E_e} = -E_{e1} R_e b_e \left(b_e \frac{\partial}{\partial V}[(V - E_e) P_0] + P_0\right). \tag{75}$$

As can be seen from Eqs. (73) and (74), the response to rate and amplitude modulation contain the same functional forms and, together with those of synaptic reversal modulation, comprise four distinct functional cases.

The high-frequency behavior for the case of conductance-based synaptic drive has the same general form (see Appendix B 1) as the current-noise case except that the voltage-dependent variance must be evaluated at V_{th}

$$\hat{r}_\alpha \simeq e^{-i\pi/4} \sqrt{\frac{\sigma_0^2(V_{\text{th}})}{\omega \tau_0}} \left.\frac{\partial F_\alpha}{\partial V}\right|_{\text{th}} - F_\alpha|_{\text{th}}. \tag{76}$$

Thus there is no qualitatively new behavior for the case of conductance fluctuations. This equation allows for the asymptotic firing-rate modulation for arbitrary drive terms to be directly calculated in terms of derivatives of P_0 at V_{th} which can in turn be related to the steady-state firing rate. The exact forms are straightforward to derive and will not be given here; nevertheless, it is worth briefly examining the types of possible behavior.

Because each of the F_α equations (73)–(75) are nonzero when evaluated at V_{th}, all of the modulations show a sustained response at high-frequency. This is consistent with variance modulation [33] in the presence of current noise in Eq. (35) because R_e, b_e, and E_e all appear in the diffusion term of the Fokker-Planck equation. To see a decaying response at high frequency an appropriately balanced, combined input must occur, such as the sum of Eqs. (73) and (74) with $R_{e1} b_e = -2 b_{e1} R_e$. This combination reveals the effect of conductance modulation centered around the reversal potential for excitation, which decays with the reciprocal of the square-root of frequency.

B. Nonlinear IF models with conductance noise

There is also little new qualitative behavior for nonlinear IF models. Defining the Langevin equation

$$C\frac{dV}{dt} = g_L(E_L - V) + g_L\psi_L + I_{\text{syn}}, \tag{77}$$

where ψ_L is the spike-generating current and I_{syn} is the conductance-based drive defined for excitation in Eq. (61). Using the definitions (64) and (65) the current operator can be written

$$\mathcal{J} = \frac{E - V + \psi}{\tau} - \frac{\partial}{\partial V}\frac{\sigma^2}{\tau}, \tag{78}$$

where the redefinition $\psi = \tau\psi_L/\tau_L$ takes into account the effective shift in threshold due to the conductance change and allows the following to be written in a similar form to the current-noise case. The equations for the steady state are

$$-\frac{\partial J_0}{\partial V} = r_0[\delta(V - V_{\text{th}}) - \delta(V - V_{\text{re}})], \tag{79}$$

$$-\frac{\partial P_0}{\partial V} = \frac{\tau_0}{\sigma_0^2}\left[\left(\frac{(V - E_0')}{\tau_0'} - \frac{\psi}{\tau_0}\right)P_0 + J_0\right] \tag{80}$$

and for the time-dependent case are

$$-\frac{\partial \hat{J}_\alpha}{\partial V} = i\omega\hat{P}_\alpha + \hat{r}_\alpha[\delta(V - V_{\text{th}}) - \delta(V - V_{\text{re}})], \tag{81}$$

$$-\frac{\partial \hat{P}_\alpha}{\partial V} = \frac{\tau_0}{\sigma_0^2}\left[\left(\frac{(V - E_0')}{\tau_0'} - \frac{\psi}{\tau_0}\right)\hat{P}_\alpha + \hat{J}_\alpha + F_\alpha\right]. \tag{82}$$

Both pairs of equations are similar to the current-based case and, furthermore, the high-frequency asymptotics can be shown (see Appendix B 2) to be of exactly the same form as that given in Eq. (46).

Before deriving the scaling of the high-frequency modulations for R_e, b_e, and E_e it is noted that for all these cases the terms appearing in F_α in Eqs. (73)–(75) may be written

$$F_{xy} = \lambda\Delta\frac{\Delta^x}{\Delta^y}\frac{\partial^x}{\partial V^x}[(V - E_e)^y P_0], \tag{83}$$

where $x=0$ or 1, $y=0$, 1 or 2 and λ has units of rate and depends on which parameter is being modulated. Before concluding this section, the results for the exponential and algebraic IF models are quoted.

C. Exponential integrate and fire model

For the EIF model $m = \omega\tau_L\Delta_T/\psi_L$. On rewriting F_{xy} in terms of m, expanding to leading order and performing the integration (46) the corresponding contribution to the firing rate modulation is

$$\hat{r}_{xy} \simeq i(-1)^x\lambda r_0\tau_L\frac{\log^y(\omega\tau_L)}{\omega\tau_L}, \tag{84}$$

to leading order. Hence the response due to R_e and b_e modulation decay as $\log^2(\omega\tau_L)/\omega\tau_L$, which is marginally slower than the case of synaptic noise modulation for the EIF given in Eq. (52). However, a combined modulation with $\mathcal{R}_{e1}b_e = -2b_{e1}R_e$, equivalent to a pure conductance modulation, scales as $\log(\omega\tau_L)/\omega\tau_L$ which is the same as the current-noise case of Eq. (52). It should be noted that the modulation of the spike-generating parameters is also unchanged.

D. Algebraic integrate and fire model

For AIF models driven by conductance-based synaptic fluctuations

$$\psi_L \simeq \Delta_T\left(\frac{V - V_T}{\Delta_T}\right)^k, \quad m = \frac{\omega\tau_L}{(k-1)}\left(\frac{V - V_T}{\Delta_T}\right)^{1-k} \tag{85}$$

and $P_0 \simeq r_0\tau_L/\psi_L$. The corresponding rate modulations can be separated into three distinct cases; for $x=0$,

$$\hat{r}_{0y} \simeq -\lambda r_0\tau_L\Gamma\left(\frac{2k - y - 1}{k - 1}\right)\left(\frac{k-1}{i\omega\tau_L}\right)^{(k-y)/(k-1)} \tag{86}$$

to leading order; for $x=1$ and $k \neq y$,

$$\hat{r}_{1y} \simeq \lambda r_0\tau_L(k - y)\Gamma\left(\frac{2k - y}{k - 1}\right)\left(\frac{k-1}{i\omega\tau_L}\right)^{(k-y+1)/(k-1)} \tag{87}$$

to leading order; and finally for $x=1$ and $k=y=2$,

$$\hat{r}_{12} \simeq \frac{4\lambda r_0\tau_L}{(\omega\tau_L)^2}\left(\frac{E_e - V_T}{\Delta_T}\right) \tag{88}$$

to leading order. For this last case, the sign would be reversed (assuming $V_T > E_i$) for modulation of the inhibitory reversal potential.

V. DISCUSSION

A simple and efficient method has been introduced for the numerical calculation of the response properties of linear and nonlinear integrate-and-fire models. The first-order response properties are an essential component of the analysis of the single-neuron response function and the categorization of the dynamic states of recurrent neuronal networks and so the method should facilitate considerably the quantitative analysis of temporal phenomena in neural tissue.

The numerical approach was complemented by the derivation of analytical forms for the high-frequency asymptotics for each of the cases, extending the known results for current and variance modulation for the LIF and EIF [7,29,31] to that of conductance modulation, modulation of the spike-generating parameters for the EIF and modulations of the parameters for IF models with a conductance-based implementation of the synaptic noise. Though for the EIF the $1/\omega$ decay was tempered by logarithmic terms, it is fair to say that no significantly new qualitative behavior was seen for conductance-based drive in comparison to current-based implementations of synaptic fluctuations: The Gaussian or effective time-constant approximation of conductance-based drive [36,37,39] is not too different from the diffusion approximation. A summary of the high-frequency behavior is provided in Table I.

A. Modulations of EIF models with finite thresholds

In the numerical evaluation or simulation of exponential IF models a finite threshold (here $V_{\text{th}}=0$ mV) must be chosen

TABLE I. Summary of results for the high-frequency response to various forms of parameter modulation for the integrate-and-fire models considered in this paper. The relevant equation numbers are provided and, where results have also been presented previously, the appropriate references are given. It can be noted that the frequency appears only in the form $i\omega\tau_0$. Hence each power of frequency brings with it a phase shift of $\pi/2$. Roots or fractional powers of i such as $1/i^{m/n}$ should therefore be interpreted as $e^{-i\pi m/2n}$. This is true for the argument of the logarithm terms also, but because only the leading order ω dependence is given in this table the constant $i\pi/2$ terms were dropped. The AIF model with $k=2$ has the same high-frequency response as the quadratic integrate-and-fire model analyzed in [31].

	Current E	Variance σ^2	Conductance g	Threshold V_T	Width Δ_T
LIF	$r_0\frac{E_1}{\sigma_0}\frac{1}{\sqrt{i\omega\tau_0}}$ Eq. (34) and Ref. [7]	$r_0\frac{\sigma_1^2}{\sigma_0^2}\left(1+\frac{(V_{\rm th}-E_0)}{\sigma_0\sqrt{i\omega\tau_0}}\right)$ Eq. (35) and Refs. [7,29]	$r_0\frac{g_1}{g_0}\frac{(E_0-V_{\rm th})}{\sigma_0\sqrt{i\omega\tau_0}}$ Eq. (36)		
EIF	$r_0\frac{1}{i\omega\tau_0}\frac{E_1}{\Delta_T}$ Eq. (51) and Ref. [31]	$r_0\frac{1}{i\omega\tau_0}\frac{\sigma_1^2}{\Delta_T^2}$ Eq. (51) and Ref. [31]	$-r_0\frac{g_1}{g_0}\frac{1}{i\omega\tau_0}\log(\omega\tau_0)$ Eq. (52)	$-r_0\frac{V_{T1}}{\Delta_T}$ Eq. (54)	$-r_0\frac{\Delta_{T1}}{\Delta_T}\log(\omega\tau_0)$ Eq. (54)
AIF	$r_0\frac{E_1}{\Delta_T}\Gamma\left(\frac{2k-1}{k-1}\right)\left(\frac{k-1}{i\omega\tau_0}\right)^{k/(k-1)}$ Eq. (58) and for $k=2$ Ref. [31]	$r_0k\frac{\sigma_1^2}{\Delta_T^2}\Gamma\left(\frac{2k}{k-1}\right)\left(\frac{k-1}{i\omega\tau_0}\right)^{(k+1)/(k-1)}$ Eq. (59) and for $k=2$ Ref. [31]	$-r_0\frac{g_1}{g_0}\frac{(k-1)}{i\omega\tau_0}$ Eq. (60)		

that is sufficiently high so as not to significantly affect the steady-state or time-dependent results. However, an examination of the derivations in Appendix B shows that the modulated response of the EIF model with a finite threshold will always cross over to LIF behavior at a sufficiently high frequency. The frequency for which the EIF asymptotics begin to lose their validity can be found by an examination of the competing frequency ω-dependent and exponential ψ-dependent terms on the left-hand side of Eq. (B14). At low voltages the ω-dependent term dominates whereas for high voltages the ψ-dependent term dominates: Equation (B18) captures the effect of both these regimes and gives the correct EIF scaling. However, if the threshold $V_{\rm th}$ occurs before the ψ term dominates then the EIF scaling argument breaks down. This occurs for frequencies greater than

$$\omega^* \sim \frac{1}{\tau_0}\exp\left(\frac{V_{\rm th}-V_T}{\Delta_T}\right). \tag{89}$$

For the parameter values investigated in this paper this crossover frequency was beyond the physiological range (i.e., significantly larger than 1000 Hz for $V_{\rm th}=0$ mV).

B. Absolute refractory period

For a short time after a spike, neurons remain nonexcitable due to a transitory inactivation of the sodium current. This absolute refractory period is often modeled by fixing the postspike voltage at the reset $V_{\rm re}$ for a duration $\tau_{\rm ref}$. Such a refractory period can be straightforwardly accommodated in the framework developed in this paper. The central difference to the nonrefractory case is seen in the current conservation equation (5) which becomes

$$J_{\rm ref}(V_{\rm re+},t)-J_{\rm ref}(V_{\rm re-},t)=r_{\rm ref}(t-\tau_{\rm ref}). \tag{90}$$

Furthermore, the density $P_{\rm ref}$ no longer integrates to unity, as a fraction of the neurons are refractory.

The steady-state rate $r_{\rm ref0}$ and density $P_{\rm ref0}$ are simply related to the corresponding nonrefractory quantities

$$r_{\rm ref0}=\frac{r_0}{1+\tau_{\rm ref}r_0} \text{ and } \rho_0=r_{\rm ref0}P_0/r_0. \tag{91}$$

For the response to a modulation relation (90) must be taken into account, and hence the equations corresponding to Eqs. (17) and (18) are

$$-\frac{\partial\hat{J}_{{\rm ref}\alpha}}{\partial V}=i\omega\hat{P}_{{\rm ref}\alpha}+\hat{r}_{{\rm ref}\alpha}(\delta(V-V_{\rm th})-e^{-i\omega\tau_{\rm ref}}\delta(V-V_{\rm re})], \tag{92}$$

$$\mathcal{J}_0\hat{P}_{{\rm ref}\alpha}=\hat{J}_{{\rm ref}\alpha}+F_{{\rm ref}\alpha}, \tag{93}$$

where the inhomogeneous term, by virtue of its linear relation to the steady-state density, is $F_{{\rm ref}\alpha}=r_{\rm ref0}F_\alpha/r_0$. These equations can be split, integrated and solved numerically, exactly as was done for the nonrefractory case.

C. Extensions of the method

The method provides a solution to the numerical calculation of the response properties of arbitrary, one-variable IF models subject to additive or multiplicative diffusive, Gaussian white noise. It has recently been shown, for the case of nonthresholded leaky integrators, that the effects of conductance-based synaptic drive cannot be fully captured within the diffusion approximation [37,39] because the shot-noise nature of the underlying synaptic drive must be accounted for. This disparity between the diffusion approximation and full shot noise stochastic dynamics has also been identified in numerical solutions of the Fokker-Planck and master equations [40] using a third-order method distinct from the one detailed here. The development of a corresponding method, for the calculation of modulatory response functions for neurons receiving full synaptic shot noise would be a worthwhile exercise, particularly given the significantly non-Gaussian nature of synaptic fluctuations seen *in vivo* [41].

Another important biophysical component of neuronal dynamics is the activation of nonlinear, voltage-gated currents.

These underlie important aspects of the neuronal response function, like subthreshold resonance [42] and spike-frequency adaptation [43]. To account for these additional currents IF models with two or more state variables are required, with the standard approach having been to linearize the activation functions and to solve the corresponding Fokker-Planck equation using an adiabatic approximation [25–27]. The method described in this paper will allow for the full nonlinear activation of the current to be included (in the adiabatic approximation) and so allow for a more complete analysis of the dynamics of neurons with voltage-gated currents.

Finally, it should be noted that the method can be easily extended to generate higher-order terms in the expansion of the Fokker-Planck equation [i.e., beyond the linear-level response given by Eqs. (8)–(10)]. The higher-order response is an important component of the weakly nonlinear analysis required to determine the nature of oscillatory instabilities in coupled networks [7]. Their analysis promises to yield further insight into the nonlinear response [44] of populations and coupled networks to afferent synaptic drive.

ACKNOWLEDGMENTS

I am indebted to Nicolas Brunel and Vincent Hakim for valuable discussions and comments, and would like to further acknowledge Vincent Hakim for suggesting the form of the algebraic integrate-and-fire model treated here.

APPENDIX A: NUMERICAL SCHEME

To perform the integration of the coupled differential equations the voltage is discretized over the range V_{lb} to V_{th} in steps of Δ such that $V^{(k)}=V_{\mathrm{lb}}+k\Delta$ with k taking values $0,1,\ldots,n$ such that $V^{(n)}=V_{\mathrm{th}}$. It proves convenient to choose Δ such that the reset V_{re} falls on a lattice point, which will be labeled k_{re}.

The differential equations for the probability density, both for the steady state and dynamic response to modulation, are of the form

$$-\frac{\partial P}{\partial V}=GP+H. \tag{A1}$$

A straightforward implementation of an Euler scheme would not have good convergence properties, particularly for the case of nonlinear models, like the EIF. An alternative scheme which avoids these problems is found by integrating the above equation to yield

$$P^{(k-1)}=P^{(k)}\exp\int_{V^{(k-1)}}^{V^{(k)}}G(V)dV+\int_{V^{(k-1)}}^{V^{(k)}}dV\,H(V)\exp\int_{V^{(k-1)}}^{V}G(U)dU, \tag{A2}$$

where all superscripts refer to the quantity evaluated at the corresponding lattice point. On expanding G and H, in all integrals, around the value at $V^{(k)}$ to zero order in Δ, the following approximation is arrived at

$$P^{(k-1)}\simeq P^{(k)}e^{\Delta G^{(k)}}+\Delta H^{(k)}\left(\frac{e^{\Delta G^{(k)}}-1}{\Delta G^{(k)}}\right) \tag{A3}$$

with corrections of order Δ^2. It can be noted that Eq. (A3) is exact if G and H are constants. This formalism is more favorable than the standard Euler method applied to Eq. (A1) because it is not necessary that ΔG_k be small—a feature that is crucial for convergence near V_{lb} for both linear and nonlinear models, and particularly for convergence near the absolute threshold V_{th} for the nonlinear models.

Given the form of Eq. (A3) it proves convenient to define the following dimensionless quantities:

$$A^{(k)}=e^{\Delta G^{(k)}}\ \text{and}\ B^{(k)}=\frac{1}{\sigma_0^2}\frac{e^{\Delta G^{(k)}}-1}{\Delta G^{(k)}}. \tag{A4}$$

Note that if $G^{(k)}=0$ for some $V^{(k)}$ then $B^{(k)}$ takes the value $1/\sigma_0^2$ at that point. Also, the case considered here corresponds to that of current-noise models where σ_0 is a constant; for conductance-based synaptic drive σ_0 is voltage dependent, but the corresponding algorithm is nevertheless straightforward to derive.

For the steady state the discretized equations (28) and (29) with the substitution (16) are

$$j_0^{(k-1)}=j_0^{(k)}-\delta_{k,k_{\mathrm{re}}+1}, \tag{A5}$$

$$p_0^{(k-1)}=p_0^{(k)}A^{(k)}+\Delta\tau_0 j_0^{(k)}B^{(k)}, \tag{A6}$$

where $\delta_{a,b}$ is the Kronecker delta function that is unity when $a=b$ and zero otherwise. These equations are integrated backwards from $V^{(n)}=V_{\mathrm{th}}$ to $V^{(0)}=V_{\mathrm{lb}}$ with the initial conditions $j_0^{(n)}=1$ and $p_0^{(n)}=0$. The firing rate is then found by integrating the (unnormalized) probability density

$$r_0=\left(\sum_{k=0}^{n}\Delta p_0^{(k)}\right)^{-1}. \tag{A7}$$

The probability densities and steady-state currents can then be correctly normalized by multiplying by r_0:

$$P_0^{(k)}=r_0p_0^{(k)}\ \text{and}\ J_0^{(k)}=r_0j_0^{(k)}. \tag{A8}$$

The equations for the response to the modulation of some parameter α can be discretized and integrated in a similar manner using the appropriate definition for F_α. As explained in Sec. II, Eqs. (17) and (18) must be integrated twice; once with the assignment $\hat{r}_\alpha=1$, $\alpha_1=0$ and once with $\hat{r}_\alpha=0$, $\alpha_1=1$. These two cases are satisfied by the pairs of functions $\hat{\mathrm{J}}_r,\hat{p}_r$ and $\hat{\mathrm{J}}_\alpha,\hat{p}_\alpha$, respectively. Thus for the first case

$$\hat{\mathrm{J}}_r^{(k-1)}=\hat{\mathrm{J}}_r^{(k)}+\Delta i\omega\hat{p}_r^{(k)}-\delta_{k,k_{\mathrm{re}}+1}, \tag{A9}$$

$$\hat{p}_r^{(k-1)}=\hat{p}_r^{(k)}A^{(k)}+\Delta\tau_0\hat{\mathrm{J}}_r^{(k)}B^{(k)}, \tag{A10}$$

with initial conditions $\hat{\mathrm{J}}_r^{(n)}=1$ and $\hat{p}_r^{(n)}=0$, and for the second case

$$\hat{\mathrm{J}}_\alpha^{(k-1)}=\hat{\mathrm{J}}_\alpha^{(k)}+\Delta i\omega\hat{p}_\alpha^{(k)}, \tag{A11}$$

$$\hat{p}_\alpha^{(k-1)} = \hat{p}_\alpha^{(k)} A^{(k)} + \Delta\tau_0 (\hat{\mathrm{J}}_\alpha^{(k)} + f_\alpha^{(k)}) B^{(k)}, \tag{A12}$$

with initial conditions $\hat{\mathrm{J}}_\alpha^{(n)}=0$, $\hat{p}_\alpha^{(n)}=0$ and where the inhomogeneous term $f_\alpha^{(k)}=F_\alpha^{(k)}/\alpha_1$ is calculated using the correctly normalized probability density P_0. From result (24) the firing-rate modulation is given by

$$\hat{r}_\alpha = -\alpha_1 \hat{\mathrm{J}}_\alpha^{(0)} / \hat{\mathrm{J}}_r^{(0)}. \tag{A13}$$

With this quantity the correct combination of the two solutions can be found to yield the full current modulation and probability density

$$\hat{J}_\alpha^{(k)} = \hat{r}_\alpha \hat{\mathrm{J}}_r^{(k)} + \alpha_1 \hat{\mathrm{J}}_\alpha^{(k)}, \tag{A14}$$

$$\hat{P}_\alpha^{(k)} = \hat{r}_\alpha \hat{p}_r^{(k)} + \alpha_1 \hat{p}_\alpha^{(k)}. \tag{A15}$$

The MATLAB code for this example is available on request.

APPENDIX B: HIGH-FREQUENCY LIMITS

Here the asymptotic forms for the firing-rate response will be extracted for the high-frequency limit. The case of the LIF model will first be addressed, followed by the nonlinear IF models. The method is cast in a form which is applicable to both additive current noise and multiplicative conductance noise.

1. High-frequency response of the leaky IF model

In the following it is assumed that the noise strength σ_0 is voltage dependent so as to allow for both the cases of current and conductance noise to be simultaneously considered; the current-noise case being recovered by replacing $\sigma_0(V)$ by its constant value.

Starting with the modulated current (31), at threshold $\hat{P}_\alpha=0$, and so

$$\hat{r}_\alpha = -\frac{\sigma_0^2}{\tau_0}(V_{\mathrm{th}}) \left.\frac{\partial \hat{P}_\alpha}{\partial V}\right|_{\mathrm{th}} - F_\alpha(V_{\mathrm{th}}). \tag{B1}$$

To calculate the firing-rate modulation it is necessary to extract the derivative of $\hat{P}_\alpha$ at threshold. It is possible to do this without having to fully solve Eq. (26) through the laborious matching of boundary conditions, as will now be shown.

The solution of the modulation equation (12) $\hat{P}_\alpha$ can be separated into a particular integral $\hat{Q}_\alpha$ and complementary function $\hat{\phi}_\alpha$ which satisfy

$$i\omega \hat{Q}_\alpha = \mathcal{L}\hat{Q}_\alpha + \frac{\partial F_\alpha}{\partial V}, \tag{B2}$$

$$i\omega \hat{\phi}_\alpha = \mathcal{L}\hat{\phi}_\alpha, \tag{B3}$$

respectively. In the large $\omega\tau_0$ limit, Eq. (B2) yields

$$\hat{Q}_\alpha = \frac{1}{i\omega}\frac{\partial F_\alpha}{\partial V}. \tag{B4}$$

In the same limit a solution for Eq. (B3) of the form $\hat{\phi}_\alpha \propto e^{\chi}$ can be expanded in powers of χ

$$i\omega = \frac{\sigma_0^2}{\tau_0}\left(\frac{\partial \chi}{\partial V}\right)^2 + O(\chi) \tag{B5}$$

so that to leading order

$$\frac{\partial \chi_\pm}{\partial V} \simeq \pm e^{i\pi/4}\sqrt{\frac{\omega\tau_0}{\sigma_0^2}}. \tag{B6}$$

In the large $\omega\tau_0$ limit it is the growing solution χ_+ that will dominate the complementary function near the voltage threshold V_{th},

$$\hat{\phi}_\alpha = \kappa e^{\chi_+ - \chi_{\mathrm{th}}}, \tag{B7}$$

where κ is a constant to be determined and $\chi_{\mathrm{th}}=\chi(V_{\mathrm{th}})$.

The boundary conditions are now imposed, the first being that at threshold $\hat{P}_\alpha$ vanishes. From Eq. (B7) the constant κ is found to be $\kappa=-\hat{Q}_\alpha(V_{\mathrm{th}})$ which is fixed by Eq. (B4). The derivative of $\hat{P}$ at threshold required for the firing-rate modulation via Eq. (B1) may now be found. Thus

$$\left.\frac{\partial \hat{P}_\alpha}{\partial V}\right|_{\mathrm{th}} = \kappa \left.\frac{\partial \chi_+}{\partial V}\right|_{\mathrm{th}} + O\left(\frac{1}{\omega}\right), \tag{B8}$$

which, on using the result (B6) and substituting for κ, yields

$$\hat{r}_\alpha = e^{-i\pi/4}\sqrt{\frac{\sigma_0^2(V_{\mathrm{th}})}{\omega\tau_0}} \left.\frac{\partial F_\alpha}{\partial V}\right|_{\mathrm{th}} - F_\alpha(V_{\mathrm{th}}), \tag{B9}$$

from which the full range of modulated responses for the LIF in the high-frequency limit can be extracted.

2. High-frequency response of nonlinear IF models

A simple argument exists [31] for extracting the high-frequency response of the EIF model to current or noise modulation. However, for conductance modulation, or other modulations that explicitly include voltage terms, this argument must be generalized and is given here for models of the form (40).

First the scaling of the steady-state probability density as a function of the average firing rate r_0 is required. From the current equation

$$0 = \tau_0 J_0 + \frac{\partial}{\partial V}(\sigma_0^2 P_0) + (V - E_0 - \psi)P_0, \tag{B10}$$

where $\sigma_0(V)$ could be voltage dependent (to include the case of conductance-based noise) and where ψ generates the spike. For the case of current-based noise σ_0 is constant, $\tau_L=\tau_0$ and definition (48) is recovered.

From Eq. (B10) it is seen that in the large V limit the steady-state distribution scales as

$$P_0 = \frac{r_0\tau_0}{\psi} + O\left(\frac{1}{\psi^2}\right). \tag{B11}$$

For the time-dependent case the current equation is of the form

$$\tau_0 \hat{J}_\alpha = \psi \hat{P}_\alpha - \frac{\partial}{\partial V}(\sigma_0^2 \hat{P}_\alpha) - (V - E_0)\hat{P}_\alpha - \tau_0 F_\alpha, \quad \text{(B12)}$$

so that in the large V limit the firing-rate modulation $\hat{r}_\alpha = \hat{J}_\alpha(V \to \infty)$ becomes

$$\tau_0 \hat{r}_\alpha = \lim_{V \to \infty} (\psi \hat{P}_\alpha - \tau_0 F_\alpha) \quad \text{(B13)}$$

and in most cases $F_\alpha(V)$ tends to zero in this limit by virtue of Eq. (B11). Hence to calculate the rate modulation the quantity $\psi \hat{P}_\alpha$ must be found in the limit of large voltages. However, it is also the limit of large frequency that is of interest and both these terms, together with the inhomogeneous term, must be included in the analysis. Hence the Fokker-Planck equation (40) for the modulation becomes

$$i\omega\tau_0 \hat{P}_\alpha + \frac{\partial \psi \hat{P}_\alpha}{\partial V} \simeq \tau_0 \frac{\partial F_\alpha}{\partial V}. \quad \text{(B14)}$$

Dividing both sides of this equation by $\omega\tau_0/\psi$ allows for a variable m that satisfies

$$\frac{dm}{dV} = -\frac{\omega\tau_0}{\psi} \quad \text{(B15)}$$

to be defined. Note that for the limit of large voltage $m \to 0$ and for large frequencies $m \to \infty$. On substituting the variable m for the voltage V, Eq. (B14) simplifies to

$$\frac{\partial \psi \hat{P}_\alpha}{\partial m} - i\psi \hat{P}_\alpha \simeq \tau_0 \frac{\partial F_\alpha}{\partial m}. \quad \text{(B16)}$$

On multiplying by $e^{-(i+s)m}$ where s is small and positive, integrating over the range from $m=0$ to $m=\infty$ and then setting s to zero, the following result required for Eq. (B13) is obtained

$$\lim_{V \to \infty} \psi \hat{P}_\alpha = -\lim_{s \to 0} \tau_0 \int_0^\infty dm\, e^{-(i+s)m} \frac{\partial F_\alpha}{\partial m}, \quad \text{(B17)}$$

which allows the firing-rate modulation in the high-frequency domain to be written in a pleasingly compact form:

$$\hat{r}_\alpha = \frac{1}{i} \lim_{s \to 0} \int_0^\infty dm\, e^{-(i+s)m} F_\alpha(m), \quad \text{(B18)}$$

though the expanded form of Eqs. (B17) and (B13) is sometimes easier to use.

[1] L. Lapicque, J. Physiol. Pathol. Gen. **9**, 620 (1907).
[2] R. B. Stein, Biophys. J. **5**, 173 (1965).
[3] R. B. Stein, Biophys. J. **7**, 37 (1967).
[4] B. Lindner, J. Garcia-Ojalvo, A. Neiman, and L. Schimansky-Geier, Phys. Rep. **392**, 321 (2004).
[5] A. N. Burkitt, Biol. Cybern. **95**, 1 (2006).
[6] A. N. Burkitt, Biol. Cybern. **95**, 97 (2006).
[7] N. Brunel and V. Hakim, Neural Comput. **11**, 1621 (1999).
[8] N. Brunel, J. Comput. Neurosci. **8**, 183 (2000).
[9] W. Gerstner, Neural Comput. **12**, 43 (2000).
[10] H. Risken *The Fokker-Planck Equation* (Springer-Verlag, Berlin, Heidelberg, New York, 1996).
[11] P. I. M. Johannesma, in *Neural Networks*, edited by E. R. Caianiello (Springer, New York, 1968), pp. 116–144.
[12] L. M. Ricciardi, *Diffusion Processes and Related Topics in Biology* (Springer, Berlin, Heidelberg, New York, 1977).
[13] N. Brunel, F. S. Chance, N. Fourcaud, and L. F. Abbott, Phys. Rev. Lett. **86**, 2186 (2001).
[14] N. Fourcaud and N. Brunel, Neural Comput. **14**, 2057 (2002).
[15] R. Moreno-Bote and N. Parga, Phys. Rev. Lett. **92**, 028102 (2004).
[16] R. Moreno, J. de la Rocha, A. Renart, and N. Parga, Phys. Rev. Lett. **89**, 288101 (2002).
[17] P. Lansky and V. Lanska, Biol. Cybern. **56**, 19 (1987).
[18] M. J. E. Richardson, Phys. Rev. E **69**, 051918 (2004).
[19] R. Moreno-Bote and N. Parga, Phys. Rev. Lett. **94**, 088103 (2005).
[20] G. B. Ermentrout, Neural Comput. **8**, 979 (1996).
[21] B. S. Gutkin and G. B. Ermentrout, Neural Comput. **10**, 1047 (1998).
[22] B. Lindner and A. Longtin, Neural Comput. **15**, 1761 (2003).
[23] N. Fourcaud-Trocmé, D. Hansel, C. van Vresswijk, and N. Brunel, J. Neurosci. **23**, 11628 (2003).
[24] N. Brunel and P. Latham, Neural Comput. **15**, 2281 (2003).
[25] M. J. E. Richardson, N. Brunel, and V. Hakim, J. Neurophysiol. **89**, 2538 (2003).
[26] N. Brunel, V. Hakim, and M. J. E. Richardson, Phys. Rev. E **67**, 051916 (2003).
[27] G. Gigante, M. Mattia, and P. Del Giudice, Phys. Rev. Lett. **98**, 148101 (2007).
[28] B. W. Knight, J. Gen. Physiol. **59**, 734 (1972).
[29] B. Lindner and L. Schimansky-Geier, Phys. Rev. Lett. **86**, 2934 (2001).
[30] G. Silberberg, M. Bethge, H. Markram, K. Pawelzik, and M. Tsodyks, J. Neurophysiol. **91**, 704 (2004).
[31] N. Fourcaud-Trocme and N. Brunel, J. Comput. Neurosci. **18**, 311 (2005).
[32] B. Doiron, B. Lindner, A. Longtin, L. Maler, and J. Bastian, Phys. Rev. Lett. **93**, 048101 (2004).
[33] B. Lindner, L. Schimansky-Geier, and A. Longtin, Phys. Rev. E **66**, 031916 (2002).
[34] S. Fusi and M. Mattia, Neural Comput. **11**, 633 (1999).
[35] A. Rauch, G. La Camera, H. R. Luscher, W. Senn, and S. Fusi, J. Neurophysiol. **90**, 1598 (2003).
[36] A. N. Burkitt, Biol. Cybern. **85**, 247 (2001).
[37] M. J. E. Richardson and W. Gerstner, Neural Comput. **17**, 923 (2005).
[38] A. L. Hodgkin and A. F. Huxley, J. Physiol. (London) **117**, 500 (1952).
[39] M. J. E. Richardson and W. Gerstner, Chaos **16**, 026106

(2006).
[40] D. Q. Nykamp and D. Tranchina, Neural Comput. **13**, 511 (2001).
[41] M. R. DeWeese and A. M. Zador, J. Neurosci. **26**, 12206 (2006).
[42] E. Puil, B. Gimbarzevsky, and R. M. Miura, J. Neurophysiol. **55**, 995 (1986).
[43] G. Fuhrmann, H. Markram, and M. Tsodyks, J. Neurophysiol. **88**, 761 (2002).
[44] Y. Aviel and W. Gerstner, Phys. Rev. E **73**, 051908 (2006).